

Room-temperature, mid-infrared ($\lambda=4.7 \mu\text{m}$) electroluminescence from single-stage intersubband GaAs-based edge emitters

D. P. Xu, A. Mirabedini, M. D'Souza, S. Li, and D. Botez^{a)}

Reed Center for Photonics, University of Wisconsin-Madison, Madison, Wisconsin 53706

A. Lyakh, Y.-J. Shen, and P. Zory

University of Florida, Gainesville, Florida 32611

C. Gmachl

Department of Electrical Engineering, Princeton University, Princeton, New Jersey 08544

(Received 17 June 2004; accepted 14 September 2004)

GaAs-based, single-stage, intersubband devices with active regions composed of deep quantum wells (i.e., $\text{In}_{0.3}\text{Ga}_{0.7}\text{As}$) and high AlGaAs barriers display strong room-temperature emission at $\lambda=4.7 \mu\text{m}$. The structures are grown by metalorganic chemical vapor deposition. The large energy barriers ($\sim 360 \text{ meV}$) for electrons in the upper energy level of the active region strongly suppress both the carrier leakage as well as the tunneling escape rate out of the wells. As a result, the ratio of emissions at 80 and 300 K is as low as 2.0, and thus there is considerably less need for a Bragg mirror/transmitter-type region. Devices with virtually 100% tunneling injection efficiency have been realized, and their room-temperature spectra are narrow: 25 meV full width at half maximum. These deep-well, single-stage structures are intended for use as the emitting units in two-dimensional, intersubband quantum-box lasers, or as the stages of quantum-cascade lasers for efficient, room-temperature operation in the 3–5- μm wavelength range. © 2004 American Institute of Physics. [DOI: 10.1063/1.1819518]

In the quest to achieve efficient, room-temperature (RT), continuous-wave (cw) laser operation in the mid-infrared (IR) wavelength range (i.e., 3–5 μm) one proposed approach is the use of two-dimensional arrays of unipolar quantum boxes¹ (QBs), with each QB incorporating a single-stage, intersubband-transition structure. In previous work on single-stage, unipolar devices RT intersubband emission has been reported only from InP-based structures² at a wavelength of 7.7 μm . For 30- to 40-stage GaAs-AlGaAs quantum-cascade (QC) lasers at RT, intersubband emission wavelengths shorter than 8 μm cannot be achieved, since at higher transition energies the active-region upper level is apparently depopulated via resonant tunneling between the X valleys of the surrounding AlGaAs barriers.³

We present here the realization of RT mid-IR electroluminescence emission from *single-stage* intersubband devices. The RT output power is of the same order of magnitude as that of InP-based QC structures of approximately the same wavelength. The RT emission linewidth is narrow [$\sim 25 \text{ meV}$ full width at half maximum (FWHM)] and the 80/300 K emission ratio is very low (~ 2).

Optimization studies of GaAs-based devices⁴ have shown that for thin barriers between the injector region and the active region, two effects occur which cause significant decreases in the upper-(energy) state injection efficiency: (1) a diagonal radiative transition from the injector-region ground state, g , to an active-region lower state, and (2) severe carrier leakage from the state g to the continuum. Here we show that by using GaAs-based devices with *very* deep active quantum wells (QWs), $\text{In}_{0.3}\text{Ga}_{0.7}\text{As}$ active layers sandwiched between $\text{Al}_{0.8}\text{Ga}_{0.2}\text{As}$ barriers, we can virtually suppress carrier leakage to the continuum. Furthermore, since

GaAs/AlGaAs superlattices do not need to be used on both sides of the active region, resonant tunneling cannot occur between X valleys at high transition energies, and thus RT emission in the mid-IR range becomes possible for GaAs-based devices.

The material used in the devices is grown by low-pressure metalorganic chemical vapor deposition (MOCVD) at 700°C and is essentially a single-stage structure embedded in a plasmon-enhanced n -GaAs waveguide,^{3,4} which gives an optical-mode confinement factor, Γ , of 0.48%. Shown in Fig. 1 is an electron-energy diagram for the single-stage structure and the squared wave-function moduli for the relevant energy states. As shown, the single-stage structure is composed of a superlattice injector and a double-QW

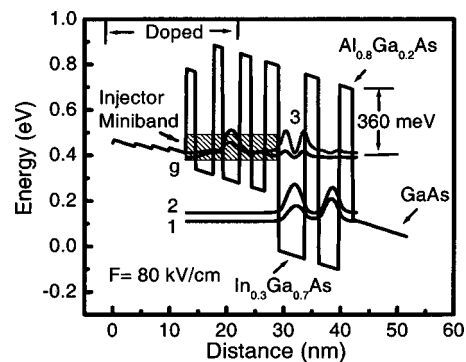


FIG. 1. Conduction-band-energy diagram of the “injector + active region” of the device when states g and $n=3$ are at resonance, under an applied electric field $F=80 \text{ kV/cm}$. Shown are the moduli squared of the relevant wave functions. The injector region is n -type doped ($4 \times 10^{17} \text{ cm}^{-3}$) over the indicated range. The layer thicknesses in nm from left to right are: 4.0/3.0/3.0/3.0/1.5/3.3/1.6/2.9/2.0/2.5/2.4/4.6/2.4/3.6/2.4; where the barriers are underlined. The first four layers are $\text{Al}_x\text{Ga}_{1-x}\text{As}$, where x is 0.02, 0.04, 0.06, and 0.08, respectively.

^{a)}Electronic mail: botez@engr.wisc.edu

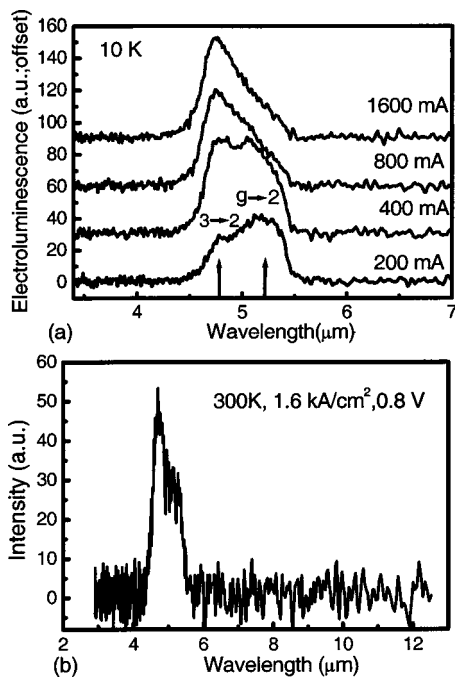


FIG. 2. Intersubband electroluminescence spectra at: (a) 10 K, for four different currents under pulsed conditions (~ 200 ns, 84 kHz). The low-energy peak is due to photon-assisted tunneling of electrons from the injector ground state (level g) to the $n=2$ state; while the high-energy peak is due to the vertical transition between the $n=3$ and $n=2$ states; (b) room temperature and 400-mA drive current (i.e., 1.6 kA/cm² current density).

(DQW) active region. The GaAs/AlGaAs superlattice injector is n type (4×10^{17} cm⁻³) over the indicated range and is designed for resonant tunneling into state $n=3$ of the active region at a field of 80 kV/cm. A step-graded region insures effective carrier flow to the miniband of the superlattice injector. The DQW active region is designed for a vertical radiative transition of 263 meV (i.e., $\lambda=4.71$ μ m), where the wells are 4.6- and 3.6-nm thick and the three barriers are each 2.4-nm thick. The $n=1$ state is separated from the $n=2$ state by approximately 32 meV, the LO-phonon energy. Since the energy splitting at resonance between the g state (of the injector) and the $n=3$ state is about 8.4 meV, the states are strongly coupled.⁵ The oscillator strength is distributed between two radiative transitions: a diagonal one from state g to the $n=2$ state, and a vertical one from the $n=3$ to the $n=2$ states.

Current confinement is provided by a 80- μ m-wide metal-contact stripe and two 1.5- μ m-deep grooves etched through the heavily doped (5×10^{18} cm⁻³) n -GaAs upper-cladding layer. The devices are 300- μ m long and mounted on Cu heat sinks. The spectra as a function of drive current and temperature are shown in Fig. 2. (Drive conditions: ~ 200 -ns-wide pulses; 84-kHz repetition rate.) At $T=10$ K and low drive levels, the electron population in the g state is much higher than that in the $n=3$ state, which causes the diagonal low-energy transition at ~ 240 meV to dominate. The emission FWHM is large (~ 35 meV), as was found by Barbieri *et al.*⁴ for thin-barrier QC devices. As the electric field increases the population of the $n=3$ state increases, which causes a shift of the emission primarily to the vertical, high-energy transition at 259 meV ($\lambda=4.78$ μ m). Increasing the temperature to 300 K [Fig. 2(b)] further increases the $n=3$ state population, such that most emission occurs from the vertical transition at $\lambda=4.7$ μ m. The emission linewidth at

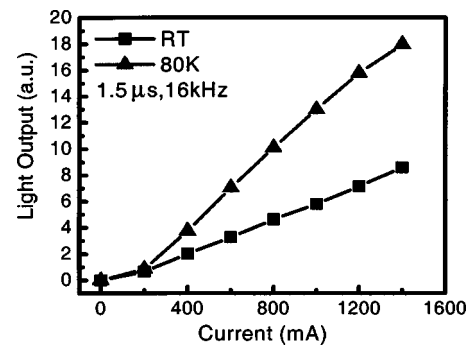


FIG. 3. Light-current curves under pulsed-drive conditions (1 μ s, 16 kHz) at 80 K and at room temperature.

4.7 μ m is estimated to be 25 meV, a value quite similar to the best RT values reported for QC devices⁶ operating at $\lambda \sim 5$ μ m.

Figure 3 shows the light-current ($L-I$) characteristics at 80 and 300 K. (Drive conditions: 1.5- μ s-wide pulsed; 16-kHz rep. rate). The outputs are of the same order of magnitude as those from InP-based QC structures emitting at the same approximate wavelength. Due both to the deep wells and the high barriers, thermionic carrier leakage to the continuum is negligible by comparison to that observed for thin-barrier GaAs/Al_{0.33}Ga_{0.67}As QC devices⁴ (i.e., the emission is *not* temperature independent). Proof of suppression of the carrier leakage is the fact that the 80/300 K emission ratio is only about 2.0, compared to typical values of ~ 3.0 for QC devices.^{2,4} Ideally, if no carrier leakage exists, the 80/300 K emission ratio should be 1.7 as dictated by Bose-Einstein statistics.¹ The strong carrier-leakage suppression occurs because the energy barrier seen by the electrons in the $n=3$ state is ~ 360 meV, a value about four times larger than for conventional 5- μ m-emitting QC devices.^{6,7} Furthermore, due to the DQW structure and the high exit barrier the tunneling escape probability of the electrons in the $n=3$ state to the continuum is strongly reduced.⁸ Thus, there is considerably less need for the Bragg mirror/transmitter region characteristic of conventional QC devices.²⁻⁸ This fact, aside from meaning less device complexity and easier fabrication, allows for the fabrication of QC devices for which backfilling^{1,7} becomes negligible at room temperature⁹ (e.g., if two structures similar to the one shown in Fig. 1 are placed

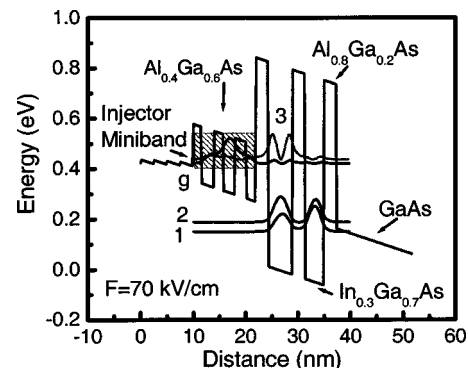


FIG. 4. Conduction-band-energy diagram for device optimized for 95% tunneling-injection efficiency from the state g to the $n=3$ state. The injector region is n -type doped just as shown in Fig. 1 for the nonoptimized device. The layer thicknesses in nm from left to right are: 2.5/2.5/2.5/2.5/1.5/2.5/1.8/2.2/2.1/1.9/2.4/4.6/2.4/3.6/2.4; where the barriers are underlined.

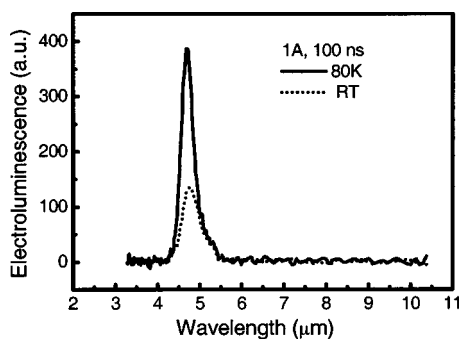


FIG. 5. Intersubband electroluminescence spectra at 80 K and at room temperature for the optimized device shown in Fig. 4.

back to back, the energy difference between the quasi-Fermi level in the doped region of the front structure and the $n=2$ state of the back structure, Δ , is quite large: ~ 150 meV.⁹ By suppressing backfilling and carrier leakage one should be able to prevent the thermal runaway which mars the room-temperature, cw performance of conventional QC devices.^{10,11}

As mentioned above, for the initial deep-well intersubband devices there is evidence of injected-carrier loss via incoherent tunneling from state g to state $n=2$. In turn the tunneling-injection efficiency, η_{in} , into state $n=3$ is $\sim 60\%$. In order to get the η_{in} value close to 100% one has to design devices for which there is strong coupling between states g and $n=3$ concomitant with weak coupling between states g and $n=2$. For InP-based devices that has been done by using a triple-QW design.⁶⁻⁸ In our case we used the structure shown in Fig. 4. By computing the overlap integrals of the wave functions for g and $n=3$ and g and $n=2$ we get a η_{in} value of 95% for an applied electric field of 75 kV/cm. (For comparison, the transition matrix elements $|z_{32}|$ and $|z_{g2}|$ are 1.76 and 0.51 nm for the optimized device versus 1.59 and 0.84 nm for the unoptimized device.) Such structures have been fabricated and tested, and the spectra are shown in Fig. 5 at a current density of 4.2 kA/cm². Now the spectra have the characteristic shape^{5,6} of intersubband transitions and

thus fully correspond to vertical transitions. The FWHM linewidths are 19 meV at 80 K and 25 meV at 300 K. [The 300-K value stays constant to the highest drive current of 1.5 A (i.e., 6.3 kA/cm² current density)]. These values are the same as, if not better than, the best values reported⁶ from 5- μ m-emitting QC devices optimized for an η_{in} value of $\sim 100\%$, and thus demonstrate that the spectral linewidths of intersubband GaAs-based devices grown by MOCVD can be as narrow as those of InP-based devices grown by molecular beam epitaxy.

In conclusion, by using deep-well, GaAs-based intersubband devices with high AlGaAs barriers we have obtained strong RT emission in the mid-IR range from single-stage intersubband emitters. Furthermore, the devices have been optimized for tunneling injection efficiency close to 100%.

This work was supported by DARPA/SPAWAR under Grant No. N66001-03-1-8900. We are also grateful to Sergey Suchalkin and Gregory Belenky for valuable technical help.

¹J-F Hsu, J-S. O, P. Zory, and D. Botez, *IEEE J. Sel. Top. Quantum Electron.* **6**, 491 (2000).

²C. Gmachl, F. Capasso, A. Tredicucci, D. L. Sivco, A. L. Hutchinson, S. N. G. Chu, and A. Y. Cho, *Appl. Phys. Lett.* **73**, 3830 (1998).

³C. Sirtori, H. Page, C. Becker, and V. Ortiz, *IEEE J. Quantum Electron.* **38**, 547 (2002).

⁴S. Barbieri, C. Sirtori, H. Page, M. Stellmacher, and J. Nagle, *Appl. Phys. Lett.* **78**, 282 (2001).

⁵C. Sirtori, F. Capasso, J. Faist, A. L. Hutchinson, D. L. Sivco, and A. Y. Cho, *IEEE J. Quantum Electron.* **34**, 1722 (1998).

⁶J. Faist, F. Capasso, C. Sirtori, D. L. Sivco, J. N. Baillargeon, A. L. Hutchinson, S. G. Chu, and A. Y. Cho, *Appl. Phys. Lett.* **68**, 3680 (1996).

⁷J. Faist, A. Tredicucci, F. Capasso, C. Sirtori, D. L. Sivco, J. N. Baillargeon, A. L. Hutchinson, and A. Y. Cho, *IEEE J. Quantum Electron.* **36**, 336 (1998).

⁸Q. K. Yang, C. Mann, F. Fuchs, R. Kiefer, K. Kohler, N. Rollbuhler, H. Schneider, and J. Wagner, *Appl. Phys. Lett.* **80**, 2048 (2002).

⁹D. Botez and D. Xu (unpublished).

¹⁰M. Hofstetter, M. Beck, T. Aellen, J. Faist, U. Oesterle, M. Illegems, E. Gini, and H. Melchior, *IEEE 18th International Semiconductor Laser Conference*, Conf. Dig. (Institute of Electrical and Electronics Engineers, Piscataway, NJ, 2002), p. 109.

¹¹A. Evans, J. S. Yu, J. David, L. Doris, K. Mi, S. Slivken, and M. Razeghi, *Appl. Phys. Lett.* **84**, 314 (2004).